Static Space Charge and Capacitance for Two-Blocking Electrodes*

J. Ross Macdonald

Texas Instruments Incorporated, Dallas 9, Texas

(Received July 28, 1958)

A one-dimensional treatment is presented of space-charge effects in materials having two charge-blocking electrodes. Especial attention is given to the situation where univalent, mobile charge carriers of only one sign can recombine bimolecularly with fixed charges of opposite sign; however, the case where noncombining charges of both signs are mobile is also included. Space-charge potential distributions and differential capacitance cannot be obtained explicitly in the general case but have been accurately calculated using a digital computer. Potential vs distance and capacitance curves are presented which illustrate dependence on applied potential, separation of electrodes, and recombination ratio. The results show features often observed experimentally for a wide variety of materials such as photoconductors, semiconductors, and insulators. The treatment is applicable for much higher applied potentials than is the case for the previously considered one blocking electrode situation with charge accumulation at the blocking electrode.

INTRODUCTION

IN a previous paper,[1] a discussion has been given of static (equilibrium) space-charge effects arising in a charge-containing material with one charge blocking and one ohmic electrode. It was assumed there that charge of only one sign was mobile but that bimolecular recombination with fixed charge of opposite sign was possible. The results obtained from a one-dimensional treatment were found for appreciable recombination to apply also to the simpler case of noncombining charges of both signs mobile.[2] In the present work, similar assumptions are made except that the material in which space-charge polarization occurs has two blocking electrodes. This case is important because, while it is always possible to make electrodes which are at least approximately blocking over a given range of applied potential, it may be considerably more difficult or impossible to ensure ohmic behavior between a metallic contact and a high-energy-gap material such as a phosphor or photoconductor.

The two-blocking electrode case differs from that with a single-blocking electrode in two major ways. First, the separation of electrodes is taken to be finite in the former and infinite in the latter case. Finite length means that effects at one electrode may interact with those at the other; thus, the physical separation of the electrodes becomes an important parameter of the problem. Second, the presence of two blocking electrodes requires that all transient charging or discharging of the system occur entirely by means of displacement rather than conduction current. Therefore, the over-all system will always be electrically neutral.

Such neutrality, which is not maintained when only one electrode is blocking, leads to much lower fields and charge concentrations than those that appear for the same applied potential difference in the one-blocking electrode case. This result means that the two-electrode solution will generally apply up to much higher applied potentials than will the one-electrode solution. For sufficiently high potentials, dielectric breakdown or high field emission will finally occur at one of the electrodes, often leading to scintillations there, and the electrode will no longer be blocking.

The case of both electrodes blocking and mobile, nonrecombining charges of both signs has been solved explicitly by Jaffé[3,4] but the result is difficult to use. This solution is formally included as a special case of the present work but here, as in the one-blocking electrode case, final integrations cannot be carried out in closed form except in limiting cases and the integrations have therefore been done herein using a digital computer.

Experimental situations where space-charge distributions of the type considered in this paper have been measured or are expected to be present are discussed in references 5 to 13 of the preceding paper.[1] In addition, the work of Gemant,[5] Thiessen, Winkel, and Herrmann,[6] Kallmann and Rosenberg,[7] and Kallmann, Kramer, and Mark[8] is pertinent. Finally, it is worth mentioning that the capacitance variation with applied potential expected in a system with one or two blocking electrodes may be useful in capacitative reactance amplifiers[9] where large nonlinearity is desirable. In particular, below a limiting frequency determined by recombination time and dimensions, such systems should show a differential capacitance which depends exponentially on bias potential over a considerable

---

[1] J. R. Macdonald, J. Chem. Phys. **29**, 1346 (1958).
[2] J. R. Macdonald and M. K. Brachman, J. Chem. Phys. **22**, 1314 (1954).

[3] G. Jaffé, Ann. Physik **16**, 217 (1933).
[4] J. R. Macdonald, J. Chem. Phys. **22**, 1329 (1954).
[5] A. Gemant, Phil. Mag. **20**, 929 (1935).
[6] Thiessen, Winkel, and Herrmann, Physik. Z. **37**, 511 (1936).
[7] H. Kallmann and B. Rosenberg, Phys. Rev. **97**, 1596 (1955).
[8] Kallmann, Kramer, and Mark, Phys. Rev. **109**, 721 (1958).
[9] A. Uhlir, Jr., Proc. Inst. Radio Engrs. **46**, 1099 (1958).

range of potential without at the same time having appreciable resistive losses.

FORMAL RESULTS

In the preceding paper, the differential equations defining space-charge distributions were solved for a general, zero-current, boundary condition and the result was then specialized to the one-blocking electrode, infinite-length case. The general solution for electric field dependence on mobile charge concentration may now be specialized for the present situation of mobile charge-containing material between two blocking electrodes. First, however, the pertinent normalized variables used will be summarized. Let

$$L_{D_1} = [\epsilon k T/4\pi e^2 N]^{\frac{1}{2}} \qquad L_{D_2} = L_{D_1}/\sqrt{2}$$

$$L_e = \theta L_{D_1} \qquad \theta = [n^*_\infty(2-n^*_\infty)]^{-\frac{1}{2}}$$

$$n^*_\infty = -(1/2R) + [(1/2R)^2 + (1/R)]^{\frac{1}{2}}$$

$$R = k_2 N/k_1 \qquad n^* = n/N \qquad p^* = p/N = [1+Rn^*]^{-1}$$

$$z = x/L_{D_1} \qquad x^* = x/L_e$$

$$L = l/L_{D_1} \qquad L^* = l/L_e = \theta^{-1}L$$

$$\psi^* = \psi/(kT/e) \qquad E^* = E/(kT/eL_e).$$

In the foregoing equations N is the initial homogeneous concentration of fixed neutral centers before any dissociation into mobile charges and fixed charges has occurred; L_{D_1} is the minimum Debye length, which is applicable for complete dissociation; L_{D_2} is the minimum Debye length when charges of both sign are mobile; and L_e is the effective Debye length (abbreviated EDL) applicable for incomplete dissociation in the one-mobile case. The separation between electrodes is l. The quantity n^*_∞ is the normalized common equilibrium value of positive and negative charge concentrations at a position where there is no space charge. The recombination ratio R involves the recombination constant k_2 and a dissociation constant k_1. It will be assumed that only negative charges of concentration n are mobile. Note that z and L are independent of R but that x^* and L^* are the distance from the left electrode and the length between the electrodes measured in terms of numbers of EDL's, which depend on R through θ and n^*_∞.

From the one-electrode case, we have

$$E^{*2} = A + 2\theta^2[n^* + \ln\{(1+Rn^*)/n^*\}], \qquad (1)$$

and

$$(1/n^*)(dn^*/dx^*) = -E^* = (d\psi^*/dx^*). \qquad (2)$$

If Eq. 2 is integrated under the condition that $n^* = n^*_\infty$ at some potential ψ^*_d, one obtains

$$n^* = n^*_\infty \exp(\psi^* - \psi^*_d) \equiv n^*_\infty \exp(\phi^*), \qquad (3)$$

where $\phi^* \equiv \psi^* - \psi^*_d$ is a new normalized potential variable. This is a reasonable boundary condition

since an applied static field will tend to accumulate mobile charge near one electrode and deplete or exhaust it in the region of the other electrode. Thus, there must be some dividing position, say x^*_d, between the electrodes where the equilibrium values of the positive and negative charge concentrations are undisturbed by the field. It is convenient to take this position as the zero of the variable ϕ^*, so that at the left positive electrode $\phi^* = \phi^*_0 \equiv \psi^*_0 - \psi^*_d$ and $\phi^* = \phi^*_e \equiv -\psi^*_d$ at the right negative electrode. Here ψ^*_0 is the total applied inner potential, including any surface and contact potential contributions. We shall always take ψ^*_0 and the left electrode positive and ψ^* will thus be zero at the right electrode, the cathode.

On using (1), (3), and $n^*_\infty = (1+Rn^*_\infty)^{-1}$, one can obtain

$$E^*(\phi^*) = \pm\sqrt{2}\theta(c_0 + n^*_\infty[\exp(\phi^*)-1]$$
$$+ \ln\{1+n^*_\infty[\exp(-\phi^*)-1]\})^{\frac{1}{2}}, \quad (4)$$

where the sign of E^* selected such that the field is directed from positive to negative charges. It will always be positive for the present case of ψ^*_0 and the left electrode positive. The quantity c_0 in (4) is an integration constant related to the constant A by $A = 2\theta^2(c_0 - n^*_\infty + \ln n^*_\infty{}^2)$. In the infinite-length, one-blocking electrode case, E^* is zero for $\psi^* = 0$ at $x^* = \infty$. Since $n^* = p^* = n^*_\infty$ at this point, ψ^*_d is identically zero and $\phi^* = \psi^*$. Thus, c_0 must be zero as well in this case; then (4) reduces to the expression found in the one-blocking electrode case. Therefore, the nonzero magnitude of c_0 in the present two-electrode case will be a sensitive function of the actual normalized length L^*, whereas this would not have been the case had the constant A been used instead of c_0.

The quantity ψ^*_d can be obtained from the condition of over-all charge neutrality in the two-electrode case. On integrating Poisson's equation from one electrode to the other, one obtains

$$\int_0^{L^*} (dE^*/dx^*)dx^* = \int_{E^*_l}^{E^*_0} dE^* = E^*_0 - E^*_l = 0, \qquad (5)$$

where the fields at the electrodes are $E^*_0 = E^*(\psi^*_0 - \psi^*_d)$ and $E^*_l = E^*(-\psi^*_d)$. The equality of these fields, as shown by (5), is the main reason for appreciable differences between the one- and two-electrode cases. The substitution of (4) into (5) and the elimination of c_0 yields the following transcendental equation for ψ^*_d,

$$\psi^*_d = \psi^*_0 - \ln\left[\frac{\ln\left\{\frac{1+[\exp(\psi^*_d)/Rn^*_\infty]}{1+\{\exp[-(\psi^*_0-\psi^*_d)]\}/Rn^*_\infty\}}\right\}}{n^*_\infty[1-\exp(-\psi^*_0)]}\right]. \qquad (6)$$

For $R = 0$ the explicit result

$$\psi^*_d = \psi^*_0 - \ln\{\psi^*_0/[1-\exp(-\psi^*_0)]\} \qquad (6')$$

is obtained. Equation (6) can also be simplified in other limiting cases. It follows from (6) that as $R \rightarrow \infty$ for fixed ψ^*_0 or as $\psi^*_0 \rightarrow 0$, ψ^*_d approaches $\psi^*_0/2$. A digital computer program has been written[10] to solve Eq. (6) or its simplified versions accurately by the Newton-Raphson iterative method for any value of R between 0 and 10^{100}.

The aforementioned results show that $\psi^*_0 > \psi^*_d \geq \psi^*_0/2$. Thus $(\psi^*_0 - \psi^*_d)$ must lie between zero and $\psi^*_0/2$. By using (3), the minimum and maximum mobile charge concentrations are $n^*_l = n^*_\infty \exp(-\psi^*_d)$ and $n^*_0 = n^*_\infty \exp(\psi^*_0 - \psi^*_d)$. When $\psi^*_d = 0$, as in the one-blocking electrode case, we have seen previously that n^*_0 reaches very large values for relatively small applied potentials. This is not the case when there are two blocking electrodes. For $R = 0$, (6') shows that $n^*_0 = \psi^*_0/[1 - \exp(-\psi^*_0)]$, which cannot appreciably exceed ψ^*_0. For $R > 0$, the maximum value of n^*_0 is approximately $n^*_{0\ max} \cong \psi^*_d - \ln R n^*_\infty$, which is always less than ψ^*_0. In addition, the maximum field $E^*_0(\phi^*_0)$ is a function of $(\psi^*_0 - \psi^*_d)$ as is n^*_0 and will not increase with applied potential as fast as in the one-blocking electrode case. The present difference arises from the condition of over-all charge neutrality and means that quite high applied potentials such as are often employed experimentally are required before breakdown occurs at an electrode or before the treatment ceases to apply because of one or more of the reasons discussed in the preceding paper.[1] The electric field in the material varies from equal maximum values at the two electrodes to a minimum value at $x^* = x^*_d$ given from (4) by $E^*(0) \equiv E^*_d = \theta(2c_0)^{\frac{1}{2}}$.

Next, integration of $d\psi^*/dx^* = d\phi^*/dx^* = -E^*$ yields the results

$$x^* = \int_{\phi^*}^{\phi^*_0} [d\phi^* / | E^*(\phi^*) |], \qquad (7)$$

$$L^* = \int_{\phi^*_l}^{\phi^*_0} [d\phi^* / | E^*(\phi^*) |], \qquad (8)$$

where $E^*(\phi^*)$ is given by (4). These equations, the implicit solutions to the static space-charge distribution problem, can only be integrated explicitly in special cases; therefore several digital computer programs have been written to carry out the necessary operations to high accuracy.[10] First, (8) is used to obtain by successive approximations the c_0 corresponding to desired values of L^*, ψ^*_0, R, and ψ^*_d. Since c_0 is often an exponential function of L^* and can vary over many orders of magnitude for moderate changes in L^*, calculation of c_0 to sufficient accuracy to make the resulting L^* within one or less percent of the desired value is a lengthy and complicated process. Next, the value of c_0 is used in (7) to yield x versus

ϕ^*, n^*, p^*, and E^*. Equality between E^*_0 and E^*_l is generally obtained to five or more significant figures and is a test of the accuracy of ψ^*_d determination. When c_0 is taken zero, the same program may be used for the one-blocking electrode case.

When $n^*_\infty [\exp(-\phi^*) - 1] \ll 1$, Eq. (7) may be reduced to

$$x^* = \int_{\phi^*}^{\phi^*_0} \{d\phi^* / [E^*_d{}^2 + 4 \sinh^2(\phi^*/2)]^{\frac{1}{2}}\}, \qquad (9)$$

which may be integrated in terms of Jacobian elliptic functions.[3,11,12] Not only is the result rather complicated but the necessary functions are not well tabulated in the ranges of most interest. Equation (9) also represents the solution of the space-charge distribution problem when charges of both signs are mobile and there is no recombination.[3] In the present case, reduction to this situation occurs formally when R is sufficiently large that the fixed charges are everywhere mobilized by recombination. Equation (7) may be integrated directly to give other approximate solutions, as was done in the one-blocking electrode case. The same result is obtained for the case $\exp(\phi^*) \gg (1 + c_0)$ as was there obtained for $\exp(\psi^*) \gg 1$ since c_0 will then be negligible. When ϕ^* is large and negative, the approximate exhaustion-depletion relation previously obtained for the one-blocking electrode case need only be modified for the present case by the transformations $\psi^*_0 \rightarrow \psi^*_0 - \psi^*_d$, $\psi^* \rightarrow \phi^*$, and the addition of c_0 inside each square root.

The maximum value of c_0 is obtained when it entirely dominates $E^*(\phi^*)$. From (8) one finds

$$c_{0\ max} = \frac{1}{2}(\psi^*_0/\theta L^*)^2 = \frac{1}{2}(\psi^*_0/L)^2. \qquad (10)$$

When $|\phi^*| \ll 1$, the sinh in (9) may be replaced by the first term of its series expansion and the integration carried out. The result is

$$x^* = \sinh^{-1}(\phi^*_0/E^*_d) - \sinh^{-1}(\phi^*/E^*_d). \qquad (11)$$

When $\phi^* = \phi^*_l$, $x^* = L^*$, and (11) becomes a transcendental equation determining c_0 in terms of L^*, ψ^*_0, ψ^*_d, and R. When c_0 is known, (11) may be used to obtain ϕ^* as a function of x^* by selecting values of ϕ^* and calculating the corresponding values of x^*. For $\phi^*_0 \gg E^*_d$, (11) gives an initial exponential drop off of ϕ^* with x^*. Since $x^*_d \cong L^*/2$ and $\phi^*_0 \cong \psi^*_0/2$ in the present case, for $\phi^* = 0$ (11) leads to

$$c_0 \cong \frac{\psi^*_0{}^2}{8\theta^2 \sinh^2(L^*/2)} = \frac{L^{*2} \cdot c_{0\ max}}{4 \sinh^2(L^*/2)}, \qquad (12)$$

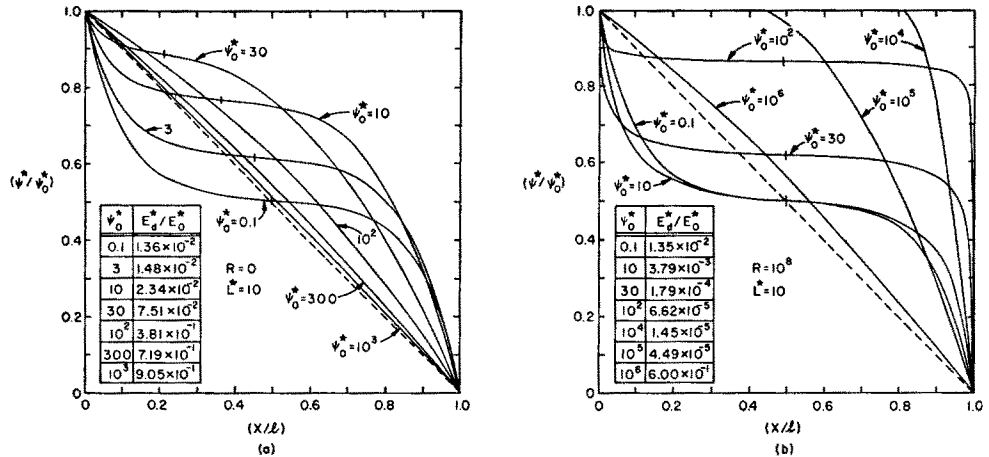which reduces to $c_{0\ max}$ when $L^* \ll 2$. Several additional approximate expressions for c_0 in various limiting cases

---

[10] Copies of this and the other IBM 650 computer programs developed for the present problem are available to any who need and can use them.

[11] R. C. Prim, Bell System Tech. J. **32**, 665 (1953).
[12] P. F. Byrd and M. D. Friedman, *Handbook of Elliptic Integrals for Engineers and Physicists* (Lange, Maxwell & Springer, Ltd., London, 1954), p. 182.

FIG. 1. Dependence of relative potential on relative position between electrodes for various normalized applied potentials and for $L^*=10$ and $R=0$, 10^8.

Fig. 1(a) table:

ψ_0^*	E_d^*/E_0^*
0.1	1.36×10^{-2}
3	1.48×10^{-2}
10	2.34×10^{-2}
30	7.51×10^{-2}
10^2	3.81×10^{-1}
300	7.19×10^{-1}
10^3	9.05×10^{-1}

Fig. 1(b) table:

ψ_0^*	E_d^*/E_0^*
0.1	1.35×10^{-2}
10	3.79×10^{-3}
30	1.79×10^{-4}
10^2	6.62×10^{-5}
10^4	1.45×10^{-5}
10^5	4.49×10^{-5}
10^6	6.00×10^{-4}

have been derived and a number of curves of c_0 dependence on L^*, R, and ψ_0^* calculated but lack of space prohibits their inclusion.

## DISCUSSION OF SPACE-CHARGE POTENTIAL CURVES

In the case of a single blocking electrode, the potential distribution curves show either charge accumulation or exhaustion-depletion regions depending upon whether the mobile charge builds up at or is withdrawn from the region of the blocking electrode by the applied potential and the resulting internal field. The two-blocking electrode potential distribution curves, on the other hand, generally show both an accumulation region near one electrode and an exhaustion-depletion region near the other. One region cannot occur without the other because of the over-all space-charge neutrality of a system in which mobile charge can neither enter nor leave the material at the electrodes. As noted in the last section, such neutrality also leads to much lower internal fields and maximum charge concentrations for a given applied potential in the present case as compared to the one-blocking electrode situation.

When both electrodes are blocking, the potential

curves depend on an additional variable, the normalized separation between the electrodes, L^*, which does not enter in the one-blocking electrode case. Since the curves depend on ψ_0^*, R, and L^* and arise from a nonlinear differential equation, they may take on a wide variety of forms, only a fraction of which can be illustrated within the scope of the present paper. Further, it is worth mentioning that if the blocking condition is partly or wholly relaxed at one but not both of the two electrodes, space-charge neutrality is no longer maintained and the potential distribution near the entirely blocking electrode will approximate the one-blocking electrode, infinite-length case, with the only difference arising from the finite length.

Figures 1 through 5 show some accurately calculated potential distribution curves. In these graphs ψ_0^* and the left electrode are always taken positive and the right electrode, the cathode, is taken to be at zero potential. Thus, accumulation regions will always appear on the left side of x_d^* (denoted by the small vertical line on the curves) and exhaustion-depletion regions on the right. The normalized abscissa, x/l, is also equal to z/L and x^*/L^*. Note that the two parts of Fig. 1 are plotted for equal L^* values but different

FIG. 2. Dependence of relative potential on relative position between electrodes for $\psi_0^*=10$, L and $L^*=10$, and various R values.
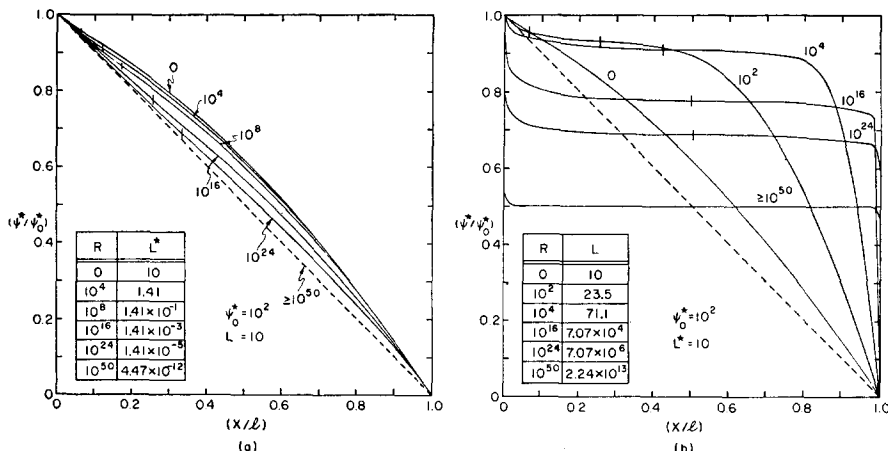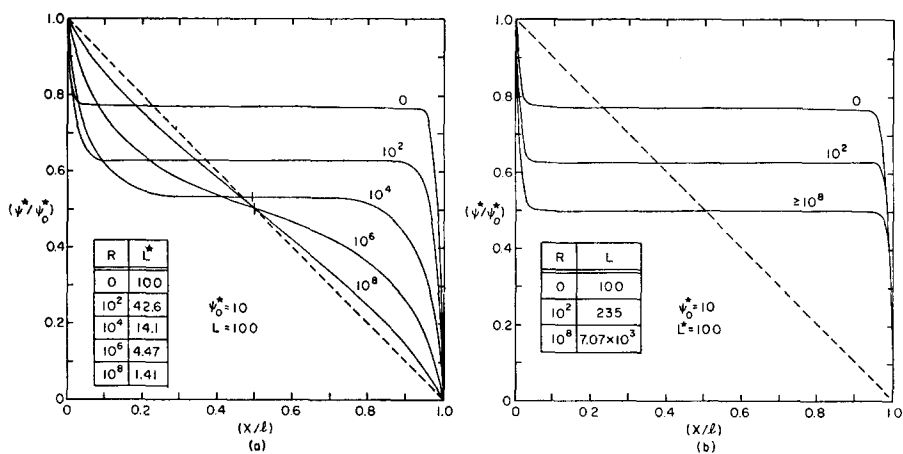
Fig. 2(a) table:

R	L^*
0	10
10^2	4.26
10^4	1.41

Fig. 2(b) table:

R	L
0	10
10^2	23.5
10^8	707
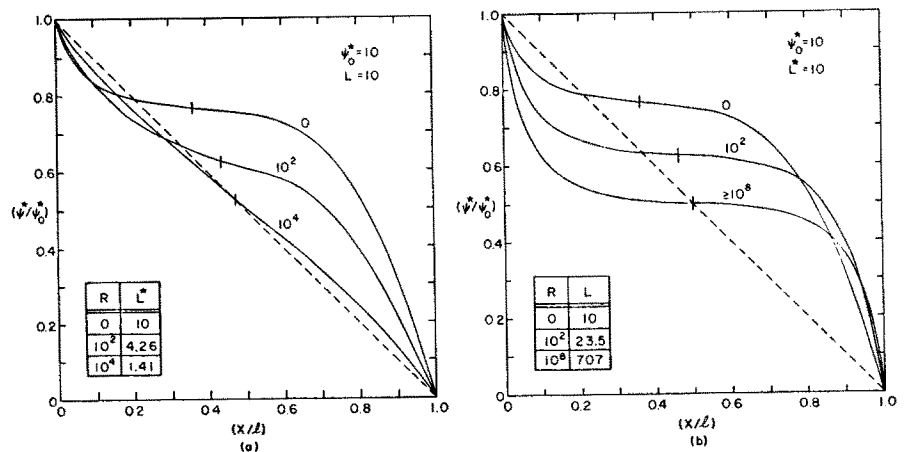
FIG. 3. Dependence of relative potential on relative position between electrodes for $\psi_0^* = 100$, L and $L^* = 10$, and various R values.

FIG. 4. Dependence of relative potential on relative position between electrodes for $\psi_0^* = 10$, L and $L^* = 100$, and various R values.
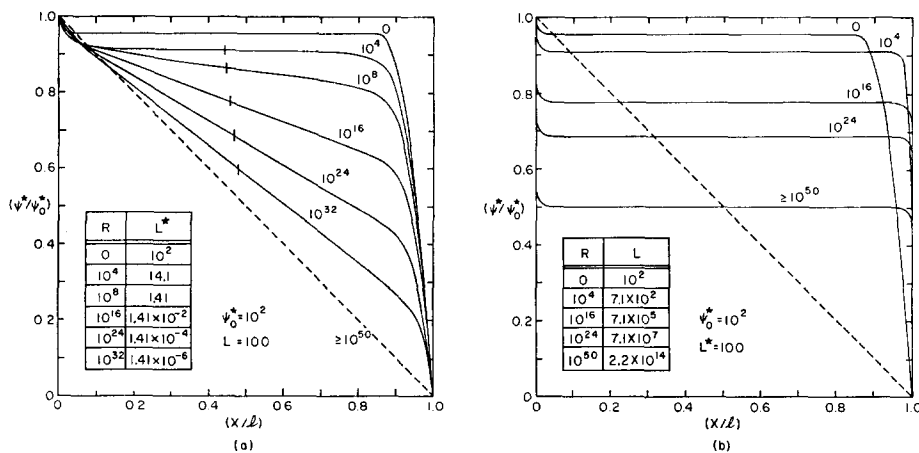

FIG. 5. Dependence of relative potential on relative position between electrodes for $\psi_0^* = 100$, L and $L^* = 100$, and various R values.

R values; on the other hand, in Figs. 2 through 5, ψ_0^* values are the same for both parts of each figure, R is used as a curve parameter, and the left and right groups are for L and L^* held constant, respectively. Thus, the left-hand curves correspond to the usual experimental case where the physical length is held constant and R is varied, for example, through changes in k_1 arising from optical activation. The

boxes in Figs. 2–5 show the values of L^* and L pertinent to the various curves; the present means of presentation allows a considerable range of these parameters to be covered as well as separating out the effects of R and length variations on curve shape.

Little detailed discussion of the various curve shapes is required since they may usually be interpreted in terms of combinations of accumulation and exhaustion-
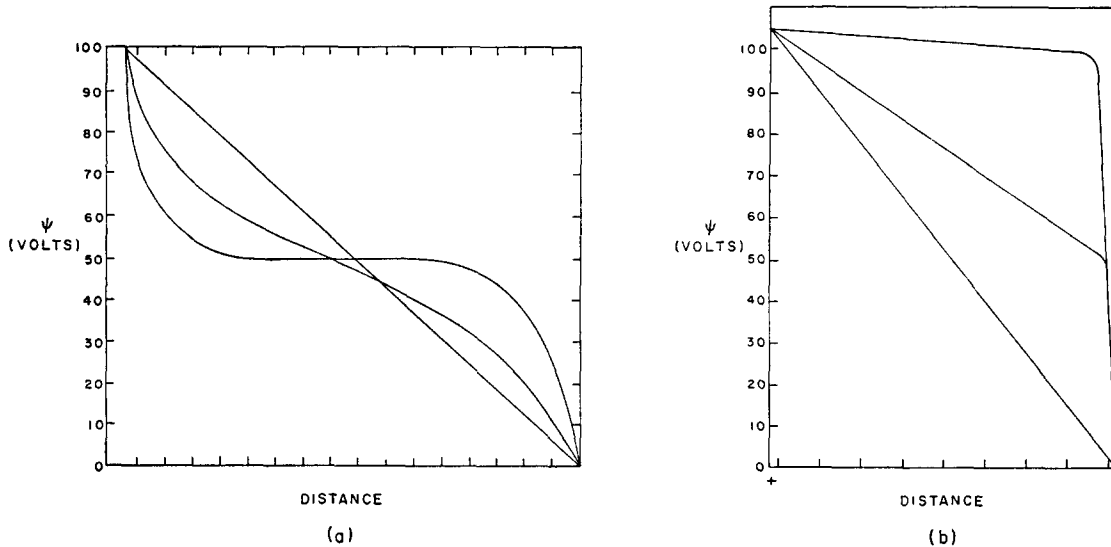
FIG. 6. Experimental potential distributions obtained during polarization build-up by Joffe[13] for (a) quartz, (b) calcite.

depletion curves of varying lengths. It will be noted that for sufficiently high applied potentials with R and L^* (and L) fixed or for sufficiently large R with ψ^*_0 and L fixed the curves approach linear dependence and $c_0 \to c_0$ max. Under these circumstances, the internal field everywhere approaches E_d max, the geometrical field, and the quantity E^*_d/E^*_0 shown in the boxes of Fig. 1 is a measure of such approach to constant internal field. This ratio tends toward unity when space charge becomes negligible. In both of the cases which lead to linear distributions, conditions are such that space charge is indeed negligible almost everywhere between the electrodes. Linear dependence for fixed ψ^*_0 and L^* is not reached for large R even though the charge density in the material may become exceptionally small because L becomes large as R increases in this case, and there is thus always room between the electrodes for the applied potential to cause some separation of charge.

Figure 5(a) is worth explicit mention because it shows that a nonlinear distribution may persist even when the number of EDL's between the electrodes becomes much less than one. The curves for $10^{10} < R \leq 10^{32}$ are made up of a nearly linear portion and a final rapid dropoff. The linear portion arises because there is no room in the actual length for an accumulation layer since L^* is less than unity. On the other hand L is large and there is room for an exhaustion layer whose width, z_e, is less than L in the present case. This exhaustion layer accounts for the final dropoff and disappears when $\exp(\psi^*_d) \ll Rn^*_\infty$. It is present even when $L^* \ll 1$ because its width in terms of the z rather than the x^* distance variable is pertinent here. For a value of L greater than z_e, an exhaustion layer can occur if R is not too great no matter what the value of L^* since L^* depends on the mobile charge

equilibrium concentration and this is immaterial in an exhaustion layer where there is no mobile charge.

Figure 6(a) and 6(b) show some experimental potential curves of Joffe[13] for heated quartz and calcite, respectively. The linear curves were observed immediately on applying the external potential while the others were measured later as polarization slowly built up. Although measurements were made at only a few positions between the electrodes in obtaining these curves and the electrodes were apparently not completely blocking (but approximate over-all neutrality was probably maintained), the curves show considerable similarity to some of the present theoretical results. Such similarity is particularly noticeable on comparing Figs. 4(a) and 6(a) and 5(a) and 6(b). It is noteworthy that Joffe explained some of his results qualitatively on the basis of recombination between mobile and fixed charges. Cohen[14] has observed rather similar potential distributions for fused quartz. Further, Kallman and Freeman have inferred that polarization of the present type is present in photoconducting phosphors,[15] and Gränicher[16] and Steinmann[16,17] have observed space-charge effects in impure ice which probably would lead, after the application of a steady potential to the material, to static space-charge distributions like those presented here. Finally, space-charge potential and charge distributions consistent with the present results are discussed in a number of the references given in the preceding paper.[1]

[13] A. F. Joffe, The Physics of Crystals (McGraw-Hill Book Company, New York, 1928).

[14] J. Cohen, J. Appl. Phys. 28, 795 (1957).

[15] H. Kallmann and J. R. Freeman, Phys. Rev. 109, 1506 (1958).

[16] A. Steinemann and H. Gränicher, Helv. Phys. Acta 30, 553 (1957).

[17] A. Steinemann, Helv. Phys. Acta 30, 581 (1957).

CHARGE AND CAPACITANCE

It is often difficult to measure static space-charge potential distributions accurately because of high impedance levels, possible small dimensions of space-charge regions, and possible surface effects. In such cases, direct measurement of the static or differential capacitance of the system as a function of an applied static bias potential can yield useful information on space charge and yet avoid difficult potential probing. It should be noted that differential capacitance measurements of this type should be made with an ac signal amplitude much smaller than the applied static potential and at frequencies sufficiently low that recombination and motional dispersion effects[18] do not appear.

In the present finite-length case, the geometrical capacitance must be considered as well as the space-charge capacitance which alone was sufficient in the infinite-length case. In the absence of free charges, the geometrical capacitance (per unit area) may be written

$$C_g = (\epsilon/4\pi l) = (\epsilon/4\pi L_e) \cdot (1/L^*). \quad (13)$$

Because of the nonlinearity inherent in the space-charge case, it will be shown later that (13) will only be directly applicable there in certain limiting situations.

A number of integrated or total charges are of interest in the two-blocking electrode case. Let

$$Q_{n_i} = e \int_{a_i}^{b_i} n(x)dx = eL_eN \int_{a^*_i}^{b^*_i} n^*(x^*)dx^*, \quad (14)$$

$$Q_{p_i} = e \int_{a_i}^{b_i} p(x)dx = eL_eN \int_{a^*_i}^{b^*_i} p^*(x^*)dx^*. \quad (15)$$

Now take $a^*_1 = 0$, $b^*_1 = x^*_d$, and $a^*_2 = x^*_d$, $b^*_2 = L^*$. The quantities Q_{n_1} and Q_{n_2} will be the total negative charge per unit electrode area (the unit area qualification will be subsequently dropped for simplicity) in the left accumulation region and the total negative charge in the right exhaustion region. Q_{p_1} and Q_{p_2} are the similar positive charges.

Now let

$$\left.\begin{aligned}
Q_n &= Q_{n_1} + Q_{n_2}, \\
Q_p &= Q_{p_1} + Q_{p_2}, \\
Q_1 &= Q_{n_1} - Q_{p_1}, \\
Q_2 &= Q_{p_2} - Q_{n_2}.
\end{aligned}\right\} \quad (16)$$

Q_n and Q_p are the total negative and positive charge magnitudes in the system; from over-all charge neutrality, they must be equal. Similarly, Q_1 and Q_2 are the excess (negative) space-charge magnitude on the accumulation side and the excess (positive) space-

18 J. R. Macdonald, Phys. Rev. **92**, 4 (1953).

charge magnitude on the exhaustion side, respectively. These quantities must also be equal. Note, however, that Q_1 and Q_n are not equal in general.

After some manipulation, we may write

$$Q_{n_1} = (kT/e)(\epsilon\theta^2/4\pi L_e)\int_0^{\psi^*_0-\psi^*_d}\frac{n^*_\infty \exp(\phi^*)d\phi^*}{|E^*(\phi^*)|}, \quad (17)$$

$$Q_{p_2}$$
$$= (kT/e)(\epsilon\theta^2/4\pi L_e)\int_{-\psi^*_d}^0 \frac{d\phi^*}{[1+Rn^*_\infty\exp(\phi^*)]|E^*(\phi^*)|} \quad (18)$$

and similar expressions for Q_{n_2} and Q_{p_1}. Q_1 may be expressed as

$$Q_1 = (kT/e)(\epsilon\theta^2/4\pi L_e)\int_0^{\psi^*_0-\psi^*_d}$$
$$\times[(-dE^*)/\theta^2dx^*][d\phi^*/|E^*(\phi^*)|]$$
$$= (kT/e)(\epsilon/4\pi L_e)\int_{E^*_d}^{E^*_0}dE^*$$
$$= (kT/e)(\epsilon/4\pi L_e)[E^*_0 - E^*_d], \quad (19)$$

where absolute value signs have been omitted since the E^*'s will always be positive. This quantity is the total charge magnitude on either electrode arising from fixed and mobile space charge between $x^* = 0$ and $x^* = x^*_d$ or between $x^* = x^*_d$ and $x^* = L^*$, but it does not include geometrical charge effects. The total electrode charge which does include such effects is

$$Q_T = (kT/e)(\epsilon/4\pi L_e)E^*_0 = (kT/e)(\epsilon/4\pi L_e)Q^*_T$$
$$= \epsilon E_0/4\pi. \quad (20)$$

The computer program that calculates x^* versus ϕ^* (Eq. 7) also calculates $Q^*_{n_1}$, $Q^*_{n_2}$, $Q^*_{p_1}$, and $Q^*_{p_2}$ by direct integration. The normalization for all charges is the same as that shown in (20); note that

$$\theta^2 \cdot (\epsilon kT/4\pi eL_e) = eL_eN.$$

For each of the Q^*'s the full integration range is split into five or more parts, thus additionally yielding the dependence of integrated charge on distance from an electrode. Further tests of the accuracy of ψ^*_d and the integrations are afforded by comparison between Q_n and Q_p obtained in this way and between the Q_1 or Q_2 value calculated from (14) and that obtained from (19). Agreement between these quantities was usually found to be better than 0.1%.

Table I shows how some of the normalized charges depend on R for $\psi^*_0 = 10$ and $L = 10$ and $L^* = 10$. In the $R = 0$ case, Q^*_n and Q^*_p must equal their zero applied-potential value $n^*_\infty L^* = L^*$, equal to 10 in the present case. When $R > 0$, however, an applied potential moves the mobile charge around, changing the amount of combined charge and relaxing the aforementioned

TABLE I. Charge dependence on R for $\psi_0^*=10$.

R	L_e/L_{D1} θ	$L=10$ E_d^*	$Q_T^*=E_0^*$	Q_1^*, Q_2^* $(E_0^*-E_d^*)$	Q_n^*, Q_p^*	$L^*=10$ E_d^*	$Q_T^*=E_0^*$	Q_1^*, Q_2^* $(E_0^*-E_d^*)$	Q_n^*, Q_p^*
0	1	8.58×10^{-2}	3.661	3.575	10	8.58×10^{-2}	3.661	3.575	10
10^2	2.35	1.016	6.578	5.562	6.346	5.48×10^{-2}	6.499	6.444	9.678
10^4	7.11	5.877	11.983	6.107	6.271	4.71×10^{-2}	10.443	10.398	13.600
10^8	70.7	70.573	71.599	1.026	1.041	4.59×10^{-2}	12.078	12.032	15.236
10^{16}	7.07×10^8	...	...	...	...	4.58×10^{-2}	12.101	12.055	15.261

requirement on Q^*_n and Q^*_p. The actual unnormalized charge is proportional to Q^*_n/θ, which decreases as R is increased. Note that for L constant c_0 approaches $c_{0\text{ max}}$ as R increases, and E^*_d therefore approaches $E^*_{d\max}=\psi^*_0/L^*=\theta(\psi^*_0/L)$, a function of R in this case. The un-normalized E_d therefore approaches ψ_0/l, the geometrical field, and is constant from one electrode to the other. On the other hand, when L^* is held constant E^*_d approaches a constant independent of R for large R [since $E^*(\phi^*)$ becomes independent of R] and E_d therefore is proportional to θ^{-1} in this limit.

The total static capacitance, including both space charge and geometrical (charge-free) contributions, is

$$C_{sT}=|Q_T/\psi_0|=(\epsilon/4\pi L_e)|E^*_0/\psi^*_0|, \quad (21)$$

while the static capacitance arising solely from space charge is

$$C_{sS}=|Q_1/\psi_0|=(\epsilon/4\pi L_e)|(E^*_0-E^*_d)/\psi^*_0|. \quad (22)$$

In the limits of zero applied potential with $L^*\ll2$, infinite applied potential, or infinite R (zero free charge), $E^*_d=E^*_0=\psi^*_0/L^*$ and $C_{sS}=0$, $C_{sT}=C_g$. When none of these conditions apply, the contribution of the geometrical capacitance to C_{sT} will be less than C_g because of the inconstancy of the electric field between the electrodes. Note that it follows from (21) that $C_{sT}^{-1}=C_{sT_1}^{-1}+C_{sT_2}^{-1}$, where C_{sT_1} and C_{sT_2} are the static capacitances associated with the accumulation and exhaustion-depletion regions, respectively.

The total differential capacitance C_{dT} may be calculated most simply from the contributions on either side of the $x^*=x^*_d$ dividing line. The accumulation and exhaustion-depletion contributions will be in series since the plane at $x^*=x^*_d$ may be replaced with an equipotential plane held at the potential ψ^*_d with no effect on the problem provided the differential capacitance is measured with an ac signal of much smaller peak amplitude than ψ^*_0. One may write

$$C_{dT}^{-1}=C_{dT_1}^{-1}+C_{dT_2}^{-1}$$
$$=(4\pi L_e/\epsilon)\{[d(\psi^*_0-\psi^*_d)/dE^*_0]+(d\psi^*_d/dE^*_l)\}. \quad (23)$$

This equation cannot be further simplified by the direct use of Poisson's equation as was done in the infinite-length problem because such simplification

would erroneously eliminate all contribution from the geometrical capacitance. The two differential terms on the right of (23) may be evaluated directly from (4), yielding, after considerable manipulation,

$$C_{dT_1}=(\epsilon\theta^2/4\pi L_e)\left\{\frac{[dc_0/d(\psi^*_0-\psi^*_d)]+(n^*_0-p^*_0)}{E^*_0}\right\}, \quad (24)$$

$$C_{dT_2}=(\epsilon\theta^2/4\pi L_e)\left[\frac{(dc_0/d\psi^*_d)+(p^*_l-n^*_l)}{E^*_l}\right], \quad (25)$$

where p^*_l and n^*_l are the normalized charge concentrations at the $x=l$ electrode and $E^*_0=E^*_l$. In the limiting cases discussed in connection with the static capacitance, C_{dT_1} and C_{dT_2} each approach $2C_g$ so that C_{dT} itself approaches C_g.

Next, it is convenient to determine the common limit C_0 of C_{dT} and C_{sT} when $\psi^*_0\to0$. To evaluate C_0, the value of c_0 given in (12) and either (21) or (23), (24), and (25) may be used. The result is

$$C_0\equiv(\epsilon/4\pi L_c)=(\epsilon/8\pi L_e)\text{ ctnh}(L^*/2)$$
$$=C_g(L^*/2)\text{ ctnh}(L^*/2), \quad (26)$$
$$L_c/L_e=2\tanh(L^*/2). \quad (27)$$

Two limiting cases are of interest. When $L^*\gg2$ so that $l\gg2L_e$, $C_0=\epsilon/8\pi L_e$. This is just one half the value found for C_0 in the infinite-length case, with the one half arising here from the presence of two blocking electrodes and space-charge regions rather than one. Alternatively, when $L^*\ll2$ so that $l\ll2L_e$, $C_0=C_g$. In this case, no space-charge separation is set up because the electrodes are much less than an effective Debye length apart.

Finally, in order to calculate C_{dT} for all conditions, the c_0 derivatives in (24) and (25) must be evaluated. We may write

$$dc_0/d(\psi^*_0-\psi^*_d)=\frac{dc_0/d\psi^*_0}{1-(d\psi^*_d/d\psi^*_0)}, \quad (28)$$

$$dc_0/d\psi^*_d=dc_0/d\psi^*_0(d\psi^*_d/d\psi^*_0)^{-1}. \quad (29)$$

The quantity $d\psi^*_d/d\psi^*_0$ may be determined in a straightforward manner from (6); since the result is very cumbersome, it will not be given. The other
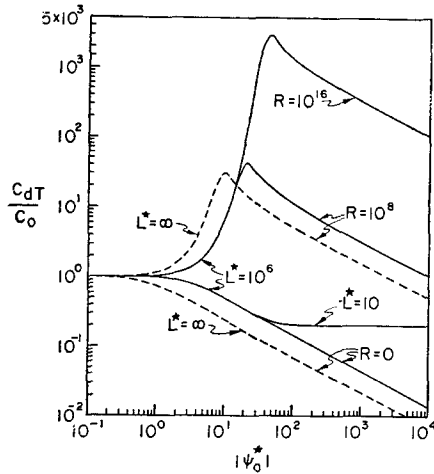
FIG. 7. Log-log plot of normalized total differential capacitance *versus* $|\psi_0^*|$ for various R and L^* values. The dashed curves ($L^* = \infty$) are for the one-blocking electrode case with an exhaustion region finally formed for large negative normalized potentials.

necessary quantity, $dc_0/d\psi^*_0$, may be obtained from (8) by differentiation under the integral sign. After simplification one finds,

$$dc_0/d\psi^*_0 = \left[\theta^2 E^*_0 \int_{\phi^*_l}^{\phi^*_0} \frac{d\phi^*}{|E^*(\phi^*)|^3} \right]^{-1}. \quad (30)$$

As a step in calculating C_{dT}/C_0, both $d\psi^*_d/d\psi^*_0$ and $dc_0/d\psi^*_0$ have been programed for IBM 650 calculation given c_0, ψ^*_0, ψ^*_d, and R. The results may then be used in a further machine program which calculates C_{dT}/C_0, C_{sT}/C_0, etc.

Figure 7 shows how C_{dT}/C_0 depends on ψ^*_0 for several R and L values. The C_{sT}/C_0 curves are similar but the peaks which occur for large R appear at greater ψ^*_0 values and are not as high as those of the C_{dT}/C_0 curves. The dashed lines in this figure are for the one-blocking electrode, $L^* = \infty$ case.[1] For $R = 0$ the main difference between the one- and two-blocking electrode curves is the horizontal separation between the two curves, equivalent to a factor of four in ψ^*_0. This factor arises from the factor of two difference in C_0 for the two cases. For $R = 10^8$ there is a factor of two ψ^*_0 difference between the two curves to the left of the peak. This difference occurs because in this region C_{dT} arises from accumulation and the potential ψ^*_0 is applied across only one accumulation layer in the one-blocking electrode case and two such layers in series in the two-blocking electrode case. This fact, plus the difference in normalization in the two situations, leads to the observed separation. Thus, when $2\psi^*_0$ is applied in the two-blocking electrode case and ψ^*_0 in the one-blocking electrode case, C_{dT} is itself one half as large in the former as compared to the latter case.

On the right of the peak, the capacitance arises from the series combination of an accumulation layer and an exhaustion-depletion layer. Since the capacitance of

an exhaustion layer progressively decreases with increasing ψ^*_0 while that of an accumulation layer increases, the exhaustion capacitance soon dominates the series combination. As ψ^*_0 increases, C_{dT}/C_0 must eventually reach C_g/C_0 when the space-charge capacitance becomes negligible compared to C_g. It is in the region where C_{dT}/C_0 is near C_g/C_0 that the c_0, $dc_0/d\psi^*_d$, and $dc_0/d(\psi^*_0 - \psi^*_d)$ terms become important. The $R = 0$, $L^* = 10$ curve shows this transition region. For $R = 10^8$ and $L^* = 10$, C_g/C_0 is reached for $\psi^*_0 \simeq 10^6$; much greater ψ^*_0 values are required to reach it for the $L^* = 10^6$ curves, for which C_g/C_0 is about 2×10^{-6}. It should be noted that although the peak of the $R = 10^{16}$ curve is much higher than that of the $R = 10^8$ curve, most of the difference arises from the dependence of C_0 on R; thus, one finds that $(C_{dT})_{16}/(C_{dT})_8$ evaluated at the two peaks is only 0.68.

In Fig. 8 the C_0 dependence on R has been eliminated by plotting C_{dT}/C_g rather than C_{dT}/C_0. The single dotted curve is for C_{sT}/C_g. Since the curves refer to constant L values, the actual physical separation between electrodes, and hence C_g remains constant as R varies. In this log–log presentation, $\log(1+R)$ is used rather than $\log R$ so that the point $R = 0$ may be included. The indicated variation in R might occur if free charge were produced in the system by the absorption of radiation. One would then expect the dissociation constant k_1 to be proportional to radiation or light intensity, I, and thus R would be proportional to I^{-1}. Then the right end of the curves would represent a low-light condition while the left boundary, $R = 0$, would correspond to infinite light intensity.

In general, these curves show that increasing L increases the maximum value of C_{dT}/C_g, while increasing ψ^*_0 primarily increases the value of R required to relax C_{dT} to C_g; the condition for such relaxation is $\exp(\psi^*_d) \ll Rn^*_\infty$. The curves show that while decreasing R (or increasing I) leads to an increase
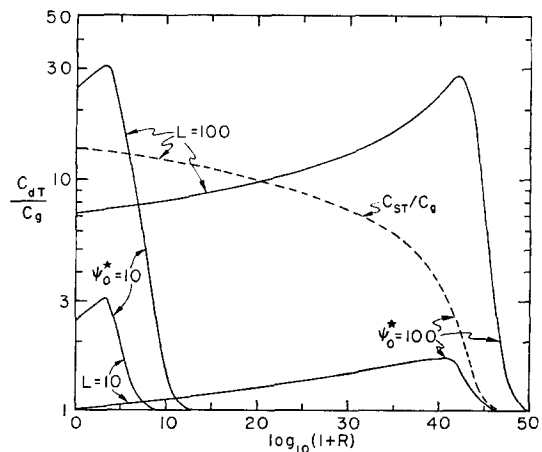

FIG. 8. Log-log plot of C_{dT}/C_g *versus* $(1+R)$ for various L and ψ_0^* values. Note that C_g, the geometrical capacitance, is independent of R. The dashed curve is for C_{sT}/C_g.

and virtual saturation of C_{sT}/C_g (which measures the total charge in the system), C_{dT}/C_g can be over-saturated so that a decrease actually occurs as R decreases.

Figure 9 shows how $(C_0-C_g)/C_g$ depends on R^{-1} for two different fixed lengths. Such a measurement might be made with a low-frequency ac signal whose peak amplitude was less than kT/e. Alternatively, it could be carried out by measuring the total charge which the system contains for smaller and smaller ψ^*_0 values and extrapolating to $\psi^*_0=0$. If the mobile charge in the system arises from optical excitation, the curves and dashed lines show that $(C_0-C_g)/C_g$ is proportional to $I^{\frac{1}{2}}$ for $C_0/C_g<1.8$. For $L\geq100$, an appreciable region also appears where $(C_0-C_g)/C_g$ is proportional to $I^{1/4}$, in agreement with (26).

When $\psi^*_0\gg1$, the differential capacitance may reach values appreciably greater than C_0. Figure 10 shows the dependence of $(C_{dT}-C_g)/C_g$ on R^{-1} for several L and ψ^*_0 values. These curves are derived from those of Fig. 8 and are plotted only for the region of greatest dependence on R. Note that the arrows indicate the pertinent R^{-1}-scales for each of the curves. Here, for $L=100$ $I^{\frac{1}{2}}$ (or $R^{-\frac{1}{2}}$) dependence (dashed lines) is evident when C_{dT}/C_g is less than about 3. In the present case, such a region of light dependence would be measurable over about four decades of light intensity.

In the preceding paper dealing with the single-blocking electrode case, the situation where the blocking electrode had to be produced artificially was discussed in some detail.[1] In the two-blocking electrode case, it may also be necessary in some cases to ensure the blocking character of the electrodes artificially, especially when the mobile charge carriers are electrons. By placing a thin film of insulating material such as
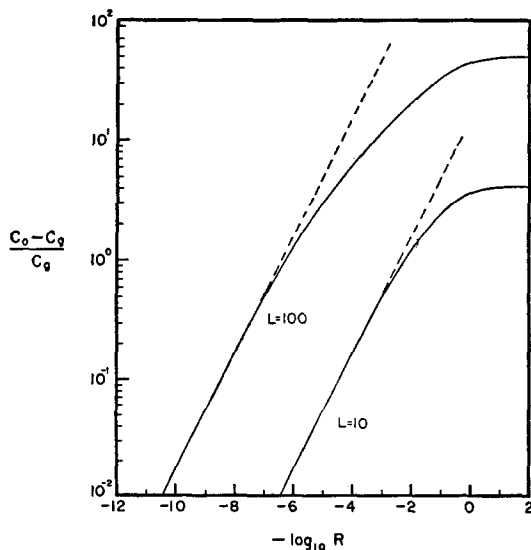

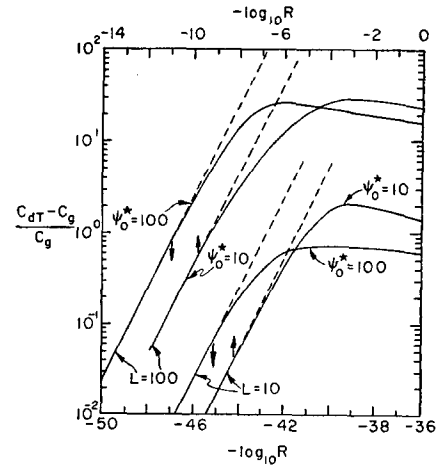FIG. 10. Log-log plot of $(C_{dT}-C_g)/C_g$ versus R^{-1} (top and bottom scales) for different ψ_0^* and L values. Dashed lines show $R^{-\frac{1}{2}}$ dependence.

Mylar or mica between the metallic electrodes and the charge-containing material, blocking can usually be well approximated. It is of course necessary to use charge-free layers sufficiently thick to avoid dielectric breakdown and tunneling.

When an external potential is applied to such a composite system, an appreciable fraction of the total potential difference may occur across the two series charge-free regions. For capacitance calculations, the potential-independent capacitances of these two regions may be combined (in series) and the combination considered as a single capacitance itself in series with the space-charge capacitance of the charge-containing material. The situation is then very similar to that in the one-blocking electrode case since Fig. 7 shows that the C_{dT}/C_0 dependence on ψ^*_0 is similar in both cases. Because of such similarity (which applies for an applied potential of polarity leading to an exhaustion region in the one-blocking electrode case but for either polarity in the two-blocking electrode case), we shall not discuss the present case in detail. Again, one would find an effective built-in potential arising from the nonlinear distribution of potential drop between the charge-free and charge-containing regions. This effective built-in potential would of course depend as before on the ratio of the capacitances of the two regions in the limit of very small applied potentials.

One final point should be mentioned. When the separation of blocking electrodes is such that $C_{dT}\gg C_g$ for given R and ψ^*_0, the geometrical capacitance can be neglected. When this is not the case and artificial blocking layers are used, the situation becomes considerably more complex. In an exact treatment, the combined space-charge, over-all geometrical, and charge-free layer capacitance should be calculated as a single problem taking into account the potential distribution from one metallic electrode to the other. In most cases of interest, however, it is likely to be

FIG. 9. Log-log plot of $(C_0-C_g)/C_g$ versus R^{-1} for two fixed lengths. The dashed lines show $R^{-\frac{1}{2}}$ dependence.

adequate to consider the boundaries between charge-free and charge-containing regions as virtual electrodes and therefore combine the (geometrical) series capacitances of the charge-free regions in series with C_{dT} (or C_{sT} if the latter is considered), noting that C_{dT} as calculated earlier in this section contains any

effects of geometrical capacitance between the virtual electrodes.

Simple Equation for Estimating the Dipole Moment of a Molecule from Solution Data

Satish Chandra Srivastava and P. Charandas

Department of Physical Chemistry, Indian Association for the Cultivation of Science, Jadavpur, Calcutta 32, India

(Received July 15, 1958)

A simple empirical equation for estimating the dipole moment of a molecule from dielectric constant measurement in solutions without any density and refraction data is suggested. The equation has been shown to be derived from an approximation of the Guggenheim-Smith equation for orientational polarization, as modified by Palit.

IT WAS pointed out by Higasi[1] that the dipole moment of a polar solute in a nonpolar solvent may be given as

$$\mu = B(\Delta\epsilon/f_2)^{\frac{1}{2}}, \qquad (1)$$

where B is a constant for the solvent (0.9 ± 0.10 esu for benzene and 1.15 ± 0.10 esu for hexene), $\Delta\epsilon$ is the difference between the dielectric constants of solution and the solvent, and f_2 is the concentration in molar fraction. Recently the range of validity of the above equation was found out by Bal Krishna and Srivastava.[2] They found that the equation holds good only for the straight portion of the dielectric constant-concentration curve and μ may be written as

$$\mu = B(d\epsilon_{12}/d f_2)^{\frac{1}{2}}, \qquad (2)$$

where $d\epsilon_{12}/d f_2$ is the slope of the straight portion of the curve.

The aim of the present note is to investigate the extent of deviation of the dipole moment values, obtained by this method, from the accepted values and to show that these are special cases of a wider equation by Guggenheim and Smith.[3,4] If the variation of ±0.10 be taken for B as pointed out by Higasi, not only is a wide range obtained for the dipole moment but also it varies with concentration, where the curve is not linear.

VARIATION OF B

However, these two variations were improved upon by Bal Krishna and Srivastava[2] by suggesting the graphical method and giving the value of B as 0.828. Though Higasi's constant gives good values for a number of solutes taken by these authors, yet the extent of variation of this constant for a large number of compounds will be clear from Tables I and II for benzene and dioxane as solvents.

BETTER EQUATION

However, a better empirical equation may be suggested as follows, if an approximate estimate of the dipole moment is required using only dielectric measurements, without solution data for refraction and density:

$$\mu = M_2^{\frac{1}{2}} A (d\epsilon_{12}/d f_2)^{\frac{1}{2}}. \qquad (3)$$

Here M_2 is the molecular weight of solute and A is a constant for the solvent, dependent upon temperature. For benzene at 25°C its value is 0.090: $d\epsilon_{12}/d f_2$ is the slope of the curve, obtained by plotting dielectric constants against weight fraction at $w_2 \rightarrow 0$. Here it is not necessary to consider only the straight portion of the curve, but an equation of the form $\epsilon_{12} = a + bw + cw^2 + \cdots$ may be written by the method of least squares and the value of $d\epsilon_{12}/d f_2$ may be obtained from it as suggested by Palit and Banerjee.[5]

DERIVATION OF THE EQUATION FROM THEORETICAL CONSIDERATIONS

The Guggenheim-Smith equation as modified by Palit,[6] for the determination of molar orientational po-

[1] K. Higasi, Bull. Inst. Phys. Chem. Research Tokyo **22**, 805 (1943).
[2] B. Krishna and K. K. Srivastava, J. Chem. Phys. **27**, 835 (1957).
[3] E. A. Guggenheim, Trans. Faraday Soc. **45**, 714 (1949).
[4] J. W. Smith, Trans. Faraday Soc. **46**, 394 (1950).

[5] S. R. Palit and B. C. Banerjee, Trans. Faraday Soc. **47**, 1299 (1951).
[6] S. R. Palit, J. Am. Chem. Soc. **74**, 3952 (1952).